Image registration algorithm-based CT-MRI images to be applied in radiotherapy of lung cancer patients with atelectasis

J.X. Wang, J. Wang, H. Lin, Y. Liang*

Department of Radiology, General Hospital of the Yangtze River Shipping, Wuhan, 430010, Hubei Province, China

► *Original article*

ABSTRACT

Background: Lung cancer (LC) is major cause of cancer-induced death. The aim of this study wasto investigate application of CT-MRI fusion images under image registration algorithm in radiotherapy for patients suffering from LC and atelectasis. *Materials and Methods:* Sixty cases of lung cancer complicated with atelectasis were randomly divided into an experimental (Exp) group and a control (Ctrl) group, and the patients were scanned by enhanced CT localization and MRI. CT-MRI images were fused by image registration algorithm, and the imaging characteristics and prognosis (curative effect, quality of life, complications) of patients were observed. *Results:* It was found that volume of the target area delimited in fusion image in Exp group was less in contrast to that in Ctrl group ($P < 0.05$). No difference existed in target encasement between the two; there was difference in values of V5 and V10 between the two. $P < 0.05$ mean lung dose in Exp group was significantly lower than that in Ctrl group. $P < 0.05$ indicated that value of cardiac V30 in Exp group was obviously less than that in Ctrl group. $P < 0.05$ demonstrated that lung recruitment in Exp group was greater when compared to that in Ctrl group after radiotherapy, while improvement of quality of life was also significantly better than that in Ctrl group, $P < 0.05$; overall response rate of radiotherapy in Exp group was slightly greater than that in Ctrl group, but difference showed no statistical significance; and no remarkable difference existed in number of cases of radiation pneumonitis between them, $P > 0.05$. *Conclusion:* Using fusion image can reduce irradiation of normal lung tissue.

INTRODUCTION

Lung cancer (LC) stands as a prevalent and lethal malignancy, causing an annual mortality of approximately 1.4 million individuals worldwide [1]. In 2010, the World Health Organization (WHO) identified tracheobronchial LC as the seventh leading cause of global mortality, marking the sole malignancy among the top ten causes of death [2]. Due to its insidious onset, nearly half of LC patients are diagnosed at an advanced stage, rendering them ineligible for surgical intervention [3]. For patients with locally advanced stage IIIA, IIIB, and certain early-stage non-small cell LC (NSCLC), as well as those with small cell LC (SCLC), a primary treatment approach involves combining radiotherapy with chemotherapy [4]. The 5-year survival rate for early-stage LC patients reaches 70%, contrasting starkly with less than 5% for those diagnosed at an advanced stage, resulting in an overall survival rate of only about 15% [5].

Over the past two decades, radiotherapy, particularly precision radiotherapy, has witnessed significant advancements in LC treatment. Precision radiotherapy, exemplified by reverse intensity-modulated radiotherapy (IMRT), has now become the cornerstone of LC treatment [6,7]. Nevertheless, the critical prerequisite for effective radiotherapy in LC lies in the accurate delineation of the target area. Presently, radiotherapy target delineation and planning are primarily reliant on CT images. However, this approach has limitations in distinguishing tumor volume, invasion extent, and metastatic lymph nodes, resulting in suboptimal gross tumor volume (GTV) definition. Central LC poses additional challenges when tumor invasion of large airways leads to obstructive pneumonia and atelectasis, causing a blending of lung and cancer tissues with similar densities, making tumor demarcation difficult [8,9].

A visible proportion of LC patients present with advanced-stage disease, co-occurring atelectasis, and, consequently, exhibit a bleak clinical prognosis with low survival rates. Concurrent or sequential chemoradiotherapy stands as a vital therapeutic approach for such patients [10]. In the course of radiotherapy, the precise delineation of the target area is of paramount concern. Furthermore, due to the reduction in the effective lung volume of patients, some CT images represent normal lung tissue,

necessitating protective measures during radiotherapy to prevent the development of radiation pneumonia (RP) [11]. Some scholars have predicted the risk of RP after radical radiotherapy for stage III NSCLC by the value of GTV / lung volume (LV), indicating that the risk factor for RP (≥ grade 2) is its ratio greater than or equal to 3.2 % [12]. Among patients with LC and atelectasis, the boundary of GTV is not clear, so it is difficult to control the delineation quality of the target area. According to the experience, the window width and window position are adjusted on the images of localization enhanced CT, and the imaging data of the patient are also referred. Many people participate in the determination of this target area. Due to the difference in the understanding of the image by each clinician, the shape and position of the drawn target area are different, and the GTV is very inaccurate [13,14]. These experiences and methods often lead to excessive range of GTV, and inevitably increase the ratio of GTV / LV because the effective volume of the patient has decreased.

The introduction of MRI diffusion-weighted imaging (DWI) has introduced a novel dimension to cancer evaluation, especially in target area determination for radiotherapy [15]. As a result, some scholars have proposed employing image fusion through a radiotherapy planning system. This involves delineating the target area on MRI images and subsequently projecting the MRI-derived target area onto CT scans using fusion algorithms, enabling dose calculations on CT scans. Nonetheless, determining the target area solely from DWI images remains challenging. The significance of image fusion becomes apparent when it complements anatomical images for adjuvant radiotherapy. While the fusion of CT and MRI images has proven beneficial in defining target areas for head and neck cancer, its application in LC has been underexplored [16]. Therefore, our study aims to fuse CT-MRI images using an image registration algorithm, evaluating its utility in the context of radiotherapy for LC and atelectasis. This approach seeks to enhance the precision of target delineation in these patients, ultimately protecting normal tissues and benefiting patient outcomes.

MATERIALS AND METHODS

General information

Sixty patients with LC complicated with atelectasis who received treatment in our Hospital between July 2021 and March 2023 were included. Patients enrolled had to satisfy all the following conditions: (1) patients with LC diagnosed by the Department of Pathology of General Hospital of the Yangtze River Shipping, including NSCLC and SCLC patients; (2) patients with comprehensive imaging data diagnosed with LC complicated with atelectasis

and the boundary of lesions on CT images could be distinguished, or patients had undergone PET-CT \ SPE CT examination; (3) patients with tumor-node-metastasis (TNM) stage III-IV; (4) patients with Karnofsky performance score (KPS) greater than 70 points; (5) patients with physical and economic conditions who met the requirements for enhanced CT and MRI simulation scan. Exclusion criteria: (1) patients with cardiac stents or other metal objects; (2) patients with poor pulmonary function that can't lie supine for a long time; (3) patients who are unwilling to cooperate with the examination and treatment; (4) patients who have received gemcitabine and gemfibrozil treatment within 30 days. The patients were assigned into two groups randomly, namely, the Exp group and the Ctrl group. The general data of the patients are shown in table 1 and figure 1.

Table 1. General information of patients.

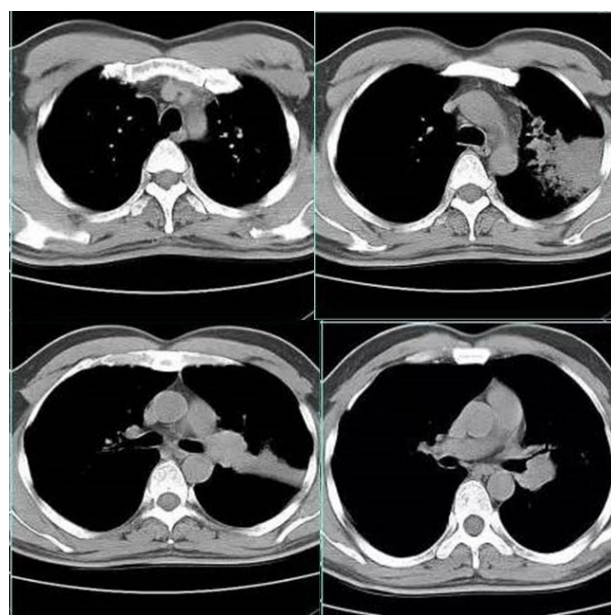| Group	Number of cases	Age	Tumor size	KPS score
Experimental group	31 cases	34 - 69 years old	3.4 - 6.6 cm	84.3 points
Control group	29 cases	40 - 66 years old	2.9 - 7.2 cm	81.5 points

Figure 1. A, B, C, D Images of patients with LC and atelectasis.

No remarkable difference was visualized in age, tumor size, and KPS score between the two groups, P>0.05. All cases and their family members had agreed on the research, and signed the written informed consent forms. The medical ethics committee of General Hospital of the Yangtze River Shipping also knew and agreed to implement it.

Experimental method
Enhanced CT localization

Before radiotherapy, the patient was asked to breathe calmly, and then the CT scan position was

performed to the patient in supine position, so that the midline of the body was located at the center of the laser positioning system (Slamtec Co., Ltd., China) to the maximum extent. According to the location of the lesion and the site of radiotherapy, the appropriate thermoplastic membrane fixation position of the head, neck, shoulder, or body was selected, and the MEDRAD-STE-ANT high pressure injector (Shenzhen Antmed Co., Ltd., China) was connected. Following intravenous injection of contrast (1.0 mL/kg, 320 mg/100 mL iodine) at the speed of 2.0 – 2.5 mL / s for 30 s, CT scanning was performed. The layer thickness was 2.5 mm, and the scanning ranged from the lower edge of the mandible to that of the liver.

MRI scan

MagOpen 2300 magnetic resonance imaging system (Shenzhen all right medical scientific co., ltd., China) was used for scanning. Scanning conditions are outlined in table 2.

Table 2. MRI scanning settings

Scan project	Scan plane	Scanning conditions
Plain scanning	Cross section T1WI	TR190, TE in phase, layer thickness 7 mm, layer spacing 1 mm, matrix size 320 × 256, excitation times: 1, layers: 18
	Cross section T2WI	TE 90, layer thickness 7 mm, layer spacing 1.5 mm, matrix size 310 × 256, excitation times: 2, layers: 18
	Cross section DWI	TE minimum, layer thickness 7 mm, layer spacing 1 mm, matrix size 256 × 256, layers 15, b = 50; 100; 200; 400; 600; 800; 1,000; 1,500; 2,000
Dynamic enhancement	Cross section LAVA	TR2.5, TE1.4, layer thickness 4 mm, flip angle 10°, matrix 256 × 160, excitation times: 2

Image transmission, registration, and fusion

Using GE16 Row Large Aperture CT Simulator (Philips, USA) to transmit images from the network to the radiotherapy planning system (Neusoft Medical, China), and the MRI image was converted to DICOM file format, which was recorded and read by the same system. The professional clinicians and radiologists participated in the image fusion of different reference points, and finally selected the best fusion image for observation and research experiments.

Mathematical model of image registration

The mathematical description of image registration can be defined as the space and gray transformation between the image for reference I_J and that to be registered I_K, and their mapping relationship can be expressed as equation 1.

$$I_K (x, y) = h[I_J (f (x, y))] \tag{1}$$

I_J (x, y) and I_K (x, y) refer to the gray value of the image for reference I_J and that to be registered I_K at the point (x, y), respectively. f(.) is a two-dimensional spatial coordinate transformation, namely, the coordinate of the image to be registered is mapped to the reference image coordinate (x', y') = f (x, y). h(.) is a one-dimensional gray transformation, which represents the gray change caused by the difference of the imaging equipment. The goal of image registration is the search for the optimal f(.) and h(.), and finally obtain the correlation between two images. Finding the optimal spatial coordinate transformation f(.) is the key to image registration. So, the registration relation can be written below.

$$I_K (x, y) = I_J (f (x, y)) \tag{2}$$

Radiotherapy

The patients were treated by intensity modulated radiation therapy. According to the CT localization image, the target area is delineated and divided into gross tumor volume (GTV), clinical target area (CTV) and planned target area (PTV). According to the requirements of tumor treatment dose and the dose limit of important organs, the treatment plan was made, and the PTV was evenly controlled between 96% and 105%, and the prescription dose was controlled at about 65Gy, 1.9Gy/ time. The limit of normal endangered organs: whole lung V20 < 26%, V5 < 55%, heart V40 <28%, V30 < 35%. Lung auscultation should be performed every day during radiotherapy, and chest radiographs should be reviewed every 14 days.

Chemotherapy

Chemotherapy was performed simultaneously on the first day of radiotherapy, and different chemotherapy schemes were adopted according to the different pathological types of patients. The chemotherapy scheme for patients with squamous cell carcinoma is as follows: 140mg/m2 paclitaxel (Yunnan Hande Bio-Tech Co., Ltd., China) is given to the patients on the first day, and 70mg/m2 nedaplatin (Yunnan Hande Bio-Tech Co., Ltd., China) is given to the patients on the second day. The chemotherapy scheme for patients with adenocarcinoma is as follows: Pemetrexed (Jiangsu Chengkang Pharmaceutical Co. Ltd., China) at a dose of 450mg/m^2 on the first day and cisplatin (Jiangsu Chengkang Pharmaceutical Co. Ltd., China) at a dose of 24mg/m^2 on the second day.

Efficacy evaluation methods

Response evaluation-criteria in solid tumors (RE-CIST) were used to assess the efficacy, and CT findings at follow-up after radiation therapy were also evaluated. Newly discovered pneumonitis in the radiation field during radiation therapy and within three months after radiation therapy was considered as RP. Radiation esophagitis was associated with pain on swallowing occurring after radiotherapy, with an NRS score ≥ 2. An increase of 10 points in Karnofsky indicated an improvement in quality of life, a

980

Int. J. Radiat. Res., Vol. 22 No. 4, October 2024

decrease of more than 10 points indicated a decrease, and an increase or decrease of less than 10 points indicated stability. The overall rate of improvement in Karnofsky score was improvement + stabilization.

Statistical methods

Data were statistically processed employing the SPSS 19.0 (IBM, USA), the data of the two groups were statistically analyzed with the rank sum test, and the P value was obtained adopting the χ^2 test or fisher's exact test, and $P < 0.05$ revealed a significant difference.

RESULTS

Imaging image after image registration algorithm

We use the image registration algorithm to process the patient's image, and the obtained image is shown in figure 2 below. It can be seen that the image quality after the image registration algorithm fusion has been significantly improved, the lung structure is clearly displayed, and the focus definition is enhanced.
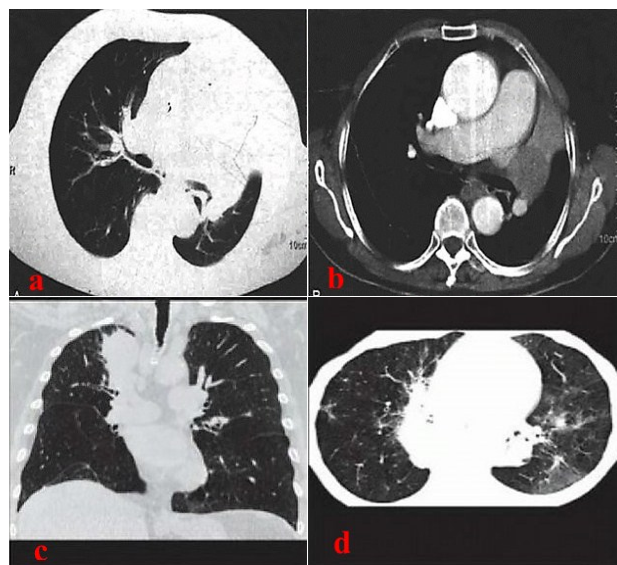

Figure 2. Imaging images after image registration algorithm. **(a)** is the CT lung window of central LC; **(b)** is the mediastinal window of enhanced CT of LC with obstructive atelectasis and **(c)** and **(d)** are the imaging images of RP.

GTV, planning target volume (PTV), and target encasement

The GTV, PTV, and target encasement of patients in the Exp and Ctrl groups are illustrated in figures 3 and 4. By observing figures 3 and 4, it is found that the delineated GTV and PTV in the Experimental group were remarkably smaller than those in Control group ($P < 0.05$). The radiation doses for patients in Experimental and Control groups were 5,385.000 cGy and 5,237.742 cGy, respectively, and no obvious difference was marked in the target encasement between the patients in Experimental and Control groups.
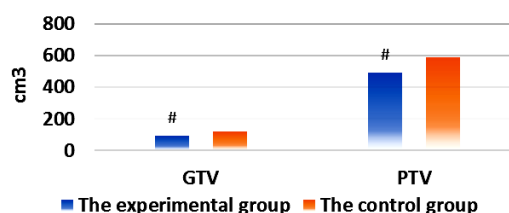

Figure 3. GTV and PTV of patients in two groups (# meant a great difference with P < 0 .05).
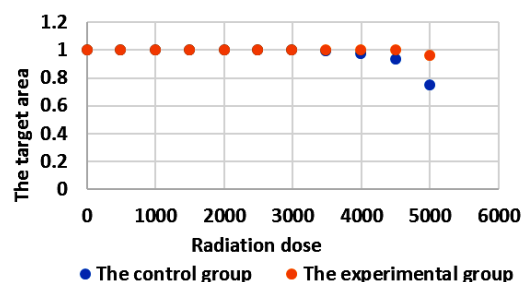

Figure 4. Target area encasement in the two groups of patients.

The dose of normal tissue

Dose for patients suffering from double lung, heart, and spinal cord tissue of Experimental group and Control group is given in figures 5 and 6. By observing figures 5 and 6, it was found that V5 and V10 of the two groups showed obvious difference in the proportion of irradiated lung volume to total lung volume ($P < 0.05$), but the value of V20 was not greatly different ($P > 0.05$); the average lung dose in the Exp. group was significantly less than that in the Ctrl group ($P < 0.05$); in the ratio of the volume of heart irradiated to total heart volume, the value of V30 in the Exp. group was remarkably lower in comparison to that in the Ctrl group ($P < 0.05$), and no significant difference was shown in the value of V40 between the two groups ($P > 0.05$); No significant difference existed in the maximum dose value of spinal cord between the two groups ($P > 0.05$).
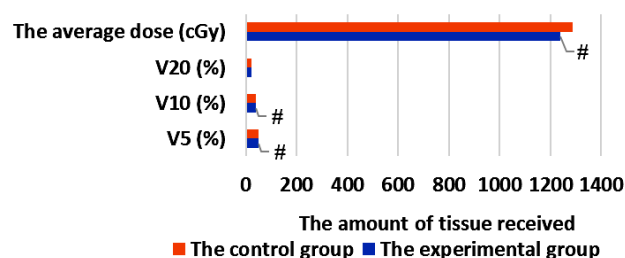

Figure 5. Dose of bilateral lung tissues. (# indicated a great difference with P < 0.05).

Lung recruitment

Lung recruitment (number of cases of recruitment, rate of recruitment) after radiotherapy in various groups is presented in figure 7. By observing figure 7, after radiotherapy, there were 25 cases of lung recruitment in the Exp group and 15 cases of lung recruitment in the Ctrl group, demonstrating obvious differences ($P < 0.05$).
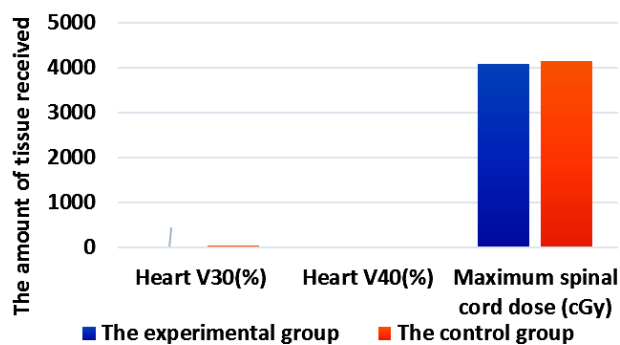
Figure 6. Dose of cardiac and spinal cord tissues (# suggested a great difference with P < 0.05).
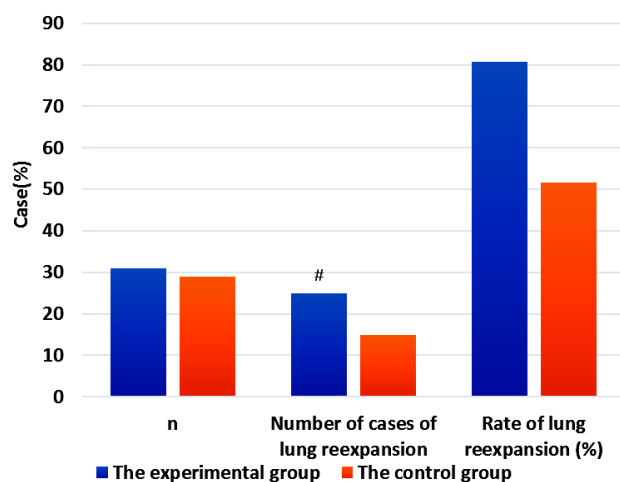

Figure 7. Lung recruitment after radiotherapy for patients in different groups (# indicated a great difference with P < 0.05).

Efficacy

The efficacy (complete remission (CR), partial remission (PR), and overall response rate) of the Exp group and the Ctrl group are explicated in figure 8. As seen in figure 8, the Exp. group had 5 cases of CR and 22 cases of PR, with the overall response rate (CR + PR) of 87.1 %; the Ctrl group had 3 cases of CR and 16 cases of PR, with the overall response rate (CR + PR) of 65.52 %, showing no remarkable difference with $P > 0.05$.
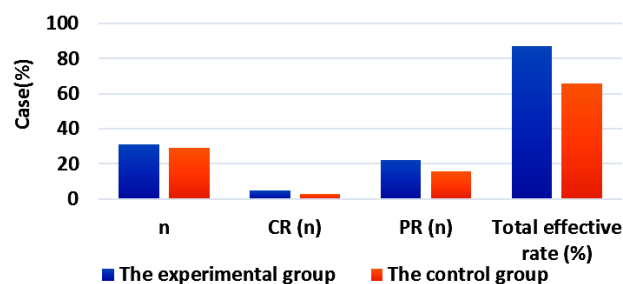

Figure 8. Efficacy of the two groups.

Improvement in life quality

The improvement of life quality after radiotherapy in the Exp. and Ctrl groups is given in figure 9. As seen in figure 9, the life quality of 18 patients in the Exp. group was improved, the life quality of 6 patients were improved stably, and that of 7 patients were decreased; 9 patients in Ctrl group

were improved, 5 patients were stable, and 15 patients were decreased; the Exp. group and the Ctrl group had KPS after radiotherapy, with the total improvement rate of 77.42 % and 48.28 %, respectively. The data differed slightly ($P < 0.05$).
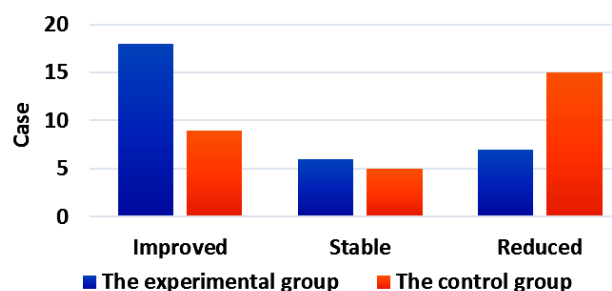

Figure 9. Improvement of quality of life after radiotherapy.

Rate of complications

The incidence of complications after radiotherapy in the Exp and Ctrl groups is summarized in table 3. Table 3 indicates a significant difference in the number of cases with RP of patients after varying groups, $P < 0.05$, and the difference showed statistical significance; while no significant difference existed in the number of cases of radiation esophagitis, $P > 0.05$.

Table 3. Incidence of complications after radiotherapy in the two groups.

	Radiation pneumonitis (RP)	Radiation esophagitis
Experimental group	3 cases	13 cases
Control group	10 cases	16 cases

DISCUSSION

Application of image registration algorithm-based CT-MRI fusion image in radiotherapy for patients with LC with atelectasis was studied. The results showed that the target volume delineated in fusion images was smaller than that delineated in enhanced CT images, and planned target volume showed the same results. The protective effect on hearts and lungs of patients in Exp. group was more significant than that in the Ctrl group with strictly complying with the limit standard of normal tissue dose. After radiotherapy, the improvement of lung re-extension and quality of life in the Exp. group was more significant than that in the Ctrl group. There existed a visible difference in the number of radioactive pneumonia cases between patients in different groups. Pulmonary artery was fused as CT and MRI of the registration markers, which reduced because of viscera activities for the impact in the quality of fused image. Based on the fusion/non-fusion images depict, a tumor volume was compared with the proportion of two effective volumes of the lung. The fusion image of target volume/lung volume significantly decreased to effectively reduce the incidence of radioactive pneumonia.

Radiotherapy stands for a main treatment method

for LC, and all aspects of the whole radiotherapy process are closely linked and interact with each other. Central LC with obstructive pneumonia or atelectasis can make it more difficult to determine the target area of LC [17]. In addition, because the respiratory amplitude of such patients is larger than that of the average person, the uncontrollability of the target area is further increased. It was reported in the literature that although the instruments and equipment for radiotherapy are continuously developing, technologies such as shape, intensity modulation, respiratory gating, and dynamic image guidance have become the key to identify and control the movement of cancer tissue with organ movement, thereby reducing the exposure of normal lung tissue [18]. However, most of the current clinical techniques are used in the implementation stage of treatment, and the systematic error caused by the delineation of the target area in the initial stage will become the key factor affecting the accuracy of radiotherapy for patients. Image registration fusion technology has attracted the attention of many clinical researchers, but the research still focuses on the implementation stage of treatment. Some scholars select the optimal image registration method by marking the difference in the coincidence of target area through different registration. It is observed that the results of central LC with cancer tissue and rumen as markers are relatively good, with the spine as the worst marker; peripheral LC with cancer tissue as the best marker, with the spine and rumen as markers are relatively poor [19, 20]. The selection of image registration markers has attracted more and more attention.

RP is a very serious complication in radiotherapy for LC. In recent years, many experts and scholars studied the occurrence and prevention of the disease from different perspectives and found that its occurrence is closely related to V5, V10, V20, the average dose of the lung, and other indicators [21]. Appel *et al*. [22] proposed that the excess of low dose region is the key factor leading to RP in intensity modulated radiotherapy. Therefore, this study strictly limited the above dosimetric indicators when formulating radiotherapy protocols. In the Exp group, the V5, V10, V20, and mean dose were 48.277 %, 38.127 %, 21.292 %, and 1,238.747 cGy, respectively; in the Ctrl group, the indicators of V5, V10, V20, and mean dose were 50.523 %, 39.64 %, 21.193 %, and 1,288.429 cGy, respectively. In the strict guarantee of normal tissue acceptance, there was still a sharp gap in the experimental data of V5, V10, and mean lung dose between the two groups, which further indicated that smaller GTV was a good way to protect lung function. The cardiac dosimetry data differed greatly, with cardiac V30 of 21.512 % and 24.045 % in the experimental and controls, respectively; no remarkable difference was revealed in V40; and in terms of the maximum dose of the spinal cord, no

visible difference was found. It may because it acts as a tandem organ with a limited maximum dose, it is generally limited to below 4,500 cGy in clinical practice, and it is difficult to achieve this dose when the target area is relatively large, and considerable cases may be asked to cause significant differences. Bezjak *et al*. [17] believe that the radiotherapy effect of lung cancer is positively correlated with the radiotherapy dose in a safe dose range. In this study, under the condition of ensuring the dose, the radiation doses to the patients in the experimental and Ctrl groups were 5,385.000 cGy and 5,237.742 cGy, respectively. This is similar to the previous results, so the dose wrapping effect formed by images fused by image registration algorithm is better. The target dose in the Exp. group was lower than that in the Ctrl group, and the data indicated that a significant protective effect was shown on the lung and heart, with better safety and better efficacy.

There are relatively few relevant studies comparing the radiotherapy efficacy and complications of LC with atelectasis using CT and DWI techniques to delimit the target area [23]. In this study, by comparing the efficacy and complications of radiotherapy after fusion of CT-MRI images, it was indicated that the lung recruitment rate in the Exp. group (25 cases) was remarkably greater than that in the Ctrl group (15 cases), and quality of life was also improved more obviously than that in the Ctrl group, *P* < 0.05. Meanwhile, the overall response rate of radiotherapy in the Exp. group was slightly greater than that in the Ctrl group without significant statistical difference, which may be related to the small number of study samples and is worthy of further study. Incidence of radiation complications in the Exp. Group was less in contrast to that in Ctrl group. In the Exp. group, 3 patients developed RP and 13 patients developed radiation esophagitis; in the Ctrl group, 10 patients developed RP and 16 patients developed radiation esophagitis. The above results suggest that fusion CT-MRI images are more accurate in delimiting the target area of LC with atelectasis, and compared with the target area delimited under enhanced CT, fusion image technology is more beneficial in protecting normal tissues from irradiation, can better complete the predetermined radiotherapy plan, reduce the risk of radiotherapy complications, and significantly enhance life quality of patients.

CONLUSION

Fusion image is of great significance for determining the boundary of cancer tissues in patients suffering from LC with atelectasis. Its application can reduce the irradiation of normal lung tissue and make patients more tolerant, which is worthy of clinical promotion. We firmly believed that CT-MRI image fusion technology would play a more

important effect in the delineation of LC targets with the rapid development of research and imaging technology.

Author Contribution: J.W.: Conceptualization, Methodology, and Data Analysis. J.W. played a key role in conceiving and designing the research, developing the methodology, and analyzing the data. J.W.: Data Collection and Visualization. J.W. was responsible for collecting and organizing the data, and also contributed to creating visual representations of the research findings. H.L.: Software Development and Experimentation; developing the necessary software tools for data analysis and conducted experiments to validate the research outcomes. Y.L.: Writing - Original Draft and Review; took the lead in drafting the initial manuscript and was also actively involved in reviewing and revising the content to ensure its accuracy and clarity.

REFERENCES

1. Schabath MB, Cote ML (2019) Cancer progress and priorities: lung cancer. *Cancer epidemiology, biomarkers & prevention, 28(10): 1563-1579.*
2. Liu H, Xie R, Dai Q, *et al*. (2023) Exploring the mechanism underlying hyperuricemia using comprehensive research on multi-omics. *Scientific Reports, 13(1): 7161.*
3. Liu H, Tang T (2023) MAPK signaling pathway-based glioma subtypes, machine-learning risk model, and key hub proteins identification. *Scientific Reports, 13(1): 19055.*
4. Ko EC, Raben D, Formenti SC (2018) The integration of radiotherapy with immunotherapy for the treatment of non–small cell lung cancer. *Clinical Cancer Research, 24(23): 5792-5806.*
5. Jacobsen MM, Silverstein SC, Quinn M, *et al*. (2017) Timeliness of access to lung cancer diagnosis and treatment: a scoping literature review. *Lung cancer, 112: 156-164.*
6. Chang Y, Xiao F, Quan H, *et al*. (2020) Evaluation of OAR dose sparing and plan robustness of beam-specific PTV in lung cancer IMRT treatment. *Radiation Oncology, 15(1): 1-12.*
7. Fornacon-Wood I, Chan C, Bayman N, *et al*. (2022) Impact of introducing intensity modulated radiotherapy on curative intent radio-

therapy and survival for lung cancer. *Frontiers in Oncology, 12: 2432.*
8. Chen N-B, Li Q-W, Zhu Z-F, *et al*. (2020) Developing and validating an integrated gross tumor volume (GTV)-TNM stratification system for supplementing unresectable locally advanced non-small cell lung cancer treated with concurrent chemoradiotherapy. *Radiation Oncology, 15: 1-12.*
9. Zhang X, Rong Y, Morrill S, *et al*. (2018) Robust optimization in lung treatment plans accounting for geometric uncertainty. *Journal of applied clinical medical physics, 19(3): 19-26.*
10. Zhao J, Zhang W, Er P, *et al*. (2020) Concurrent or sequential chemoradiotherapy after 3-4 cycles induction chemotherapy for ls-sclc with bulky tumor. *Journal of Cancer, 11(17): 4957.*
11. Li J, Fu X, Fu J (2017) Exhaled Nitric oxide is useful in symptomatic radioactive pneumonia: a retrospective study. *Mediators of Inflammation.*
12. Chai G, Yin Y, Zhou X, *et al*. (2020) Pulmonary oligometastases treated by stereotactic body radiation therapy (SBRT): A single institution's experience. *Translational Lung Cancer Research, 9(4): 1496.*
13. Kandathil A, Kay FU, Butt YM, *et al*. (2018) Role of FDG PET/CT in the eighth edition of TNM staging of non–small cell lung cancer. *Radiographics, 38(7): 2134-2149.*
14. Zhao M, Ma Y, Yang B, *et al*. (2016) A meta-analysis to evaluate the diagnostic value of dual-time-point F-fluorodeoxyglucose positron emission tomography/computed tomography for diagnosis of pulmonary nodules. *Journal of cancer research and therapeutics, 12(Special 3): C304-C308.*
15. Colletti PM (2020) Reverse phase encoding–corrected DWI Improves MRI for PET/MRI of lung cancer. *Radiological Society of North America, 701-702.*
16. Shen S, Zhang S, Liu P, *et al*. (2020) Potential role of microRNAs in the treatment and diagnosis of cervical cancer. *Cancer Genet, 248-249: 25-30.*
17. Bezjak A, Paulus R, Gaspar LE, *et al*. (2019) Safety and efficacy of a five-fraction stereotactic body radiotherapy schedule for centrally located non–small-cell lung cancer: NRG oncology/RTOG 0813 trial. *Journal of Clinical Oncology, 37(15): 1316.*
18. Liang JA, Tu CY, Hsia TC, *et al*. (2020) Effectiveness of image-guided radiotherapy for locally advanced lung cancer patients treated with definitive concurrent chemoradiotherapy. *Thoracic cancer, 11(9): 2639-2649.*
19. Yan WL, Lv JS, Guan ZY, *et al*. (2017) Impact of target area selection in 125 I odine seed brachytherapy on locoregional recurrence in patients with non-small cell lung cancer. *Thoracic Cancer, 8(3): 147-152.*
20. Abuodeh Y, Naghavi AO, Echevarria M, *et al*. (2018) Quantitatively excessive normal tissue toxicity and poor target coverage in post-operative lung cancer radiotherapy meta-analysis. *Clinical Lung Cancer, 19(1): e123-e30.*
21. Shen T, Sheng L, Chen Y, *et al*. (2020) High incidence of radiation pneumonitis in lung cancer patients with chronic silicosis treated with radiotherapy. *Journal of Radiation Research, 61(1): 117-122.*
22. Appel S, Bar J, Ben-Nun A, *et al*. (2019) Comparative effectiveness of intensity modulated radiation therapy to 3-dimensional conformal radiation in locally advanced lung cancer: pathological and clinical outcomes. *The British Journal of Radiology, 92(1097): 20180960.*
23. Zurstrassen CE, Tyng CJ, Guimarães MD, *et al*. (2020) Functional and metabolic imaging in transthoracic biopsies guided by computed tomography. *European Radiology, 30: 2041-2048.*